Journal of Vertebrate Paleontology

ISSN: (Print) (Online) Journal homepage: https://www.tandfonline.com/loi/ujvp20

A new glirid-like cricetid from the lower Oligocene of southern China

Xiao-Yu Lu, Xijun Ni & Olivier Maridet

To cite this article: Xiao-Yu Lu, Xijun Ni & Olivier Maridet (2021): A new glirid-like cricetid from the lower Oligocene of southern China, Journal of Vertebrate Paleontology, DOI: 10.1080/02724634.2021.1917587

To link to this article: https://doi.org/10.1080/02724634.2021.1917587

Journal of Vertebrate Paleontology e1917587 (10 pages)
Published with license by the Society of Vertebrate Paleontology
DOI: 10.1080/02724634.2021.1917587

ARTICLE

A NEW GLIRID-LIKE CRICETID FROM THE LOWER OLIGOCENE OF SOUTHERN CHINA

XIAO-YU LU,[1,2] XIJUN NI, [3,4,5,6]* and OLIVIER MARIDET [1,2]*
[1]Jurassica Museum, Rte de Fontenais 21, 2900 Porrentruy, Switzerland, olivier.maridet@jurassica.ch;
[2]Department of Geosciences, Earth Sciences, University of Fribourg, Chemin du Musée 6, Pérolles, 1700 Fribourg, Switzerland;
[3]Key Laboratory of Evolutionary Systematics of Vertebrates, Institute of Vertebrate Paleontology and Paleoanthropology, Chinese Academy of Sciences, Beijing 100044, PR China, nixijun@ivpp.ac.cn;
[4]CAS Center for Excellence in Life and Paleoenvironment, Beijing, 100044, PR China;
[5]CAS Center for Excellence in Excellence in Tibetan Plateau Earth Sciences, Beijing, 100104, PR China;
[6]University of Chinese Academy of Sciences, Beijing, 101408, PR China

ABSTRACT—Here we report a new cricetid s.l., *Caecocricetodon yani*, gen. et sp. nov., discovered in the early Oligocene of the Caijiachong Formation in Yunnan Province, China. The new cricetid differs from all known cricetids or stem muroids by its particular molar pattern displaying numerous crests and spurs. Our phylogenetic analysis based on a matrix including 42 taxa and 72 characters indicates that the new species has a close relationship with Paracricetodontinae, forming a monophyletic clade with *Paracricetodon* and *Trakymys*. The new cricetid also has a likely close relationship with *Pappocricetodon*. However, the genus *Pappocricetodon* is polyphyletic in our analysis. Considering the similarity of the brachydont lophodont teeth of *Caecocricetodon* and glirids, we propose that the new species underwent convergent evolution with dormice, possibly adapting to an arboreal ecological niche in Oligocene of southern China.

http://zoobank.org/urn:lsid:zoobank.org:pub:39B009F6-0EA3-4137-BC84-93022A745DCB

SUPPLEMENTAL DATA—Supplemental materials are available for this article for free at www.tandfonline.com/UJVP

Citation for this article: Lu, X.-Y., X. Ni, and O. Maridet. 2021. A new glirid-like cricetid from the lower Oligocene of Southern China. Journal of Vertebrate Paleontology. DOI: 10.1080/02724634.2021.1917587

INTRODUCTION

Cricetids, including extant hamsters, are the second most species-rich family of rodents. Among stem muroids, the first record of this family traces back to the middle Eocene of China (*Pappocricetodon antiquus* Wang and Dawson, 1994; *Palasiomys conulus* Tong, 1997). However, they only started to diversify rapidly since their arrival in Europe and North America at the beginning of the Oligocene. During the last two decades, many new extinct species and several new genera were added into the family Cricetidae s.l. With these new discoveries, some phylogenetic analyses were performed in order to better understand the origin and evolution of the family (Gomes Rodrigues et al., 2010; Maridet and Ni, 2013).

The specimens of a new cricetid rodent were discovered at Caijiachong in Yunnan Province, China (Fig. 1). The Caijiachong mammalian fossil localities lie in Yuezhou Basin, about 20 km southeast of Qujing City. Mammalian remains were discovered from at least six fossiliferous layers in the Caijiachong Formation, which is a set of sediments consisting of gray and light grayish-green sandstone or sandy mudstone and a grayish-white marlstone bed. In the past decade, abundant mammal fossils were discovered from a fossiliferous layer in the upper part of the Caijiachong Formation at the Lijiawa locality. The fossils include the earliest-known tree shrew *Ptilocercus kylin* Li and Ni, 2016, diverse primates, and several new species of cricetids s.l., such as *Paracricetops virgatoincisus* Maridet and Ni, 2013 and *Cricetops auster* Li et al., 2016 (Maridet and Ni 2013; Li and Ni, 2016; Li et al., 2016; Ni et al., 2016). The assemblage of these diverse mammals indicates an age of early Oligocene and a tropical forest environment (Maridet and Ni, 2013; Li et al., 2016; Li and Ni, 2016; Ni et al., 2016). The new cricetid reported here comes from two sites (19 and 20) near Caijiachong village. Stratigraphically the two sites are correlated to a layer higher than the lower Oligocene fossil layer of Lijiawa locality, but the two sites also yield other early Oligocene fossils such as *Cricetops auster*.

The peculiar brachydont lophodont teeth of the new species reported here resembles another family: Gliridae Thomas, 1897, the family of extant dormice. Most extinct glirid rodents are recorded in Europe where they first appear in the lower Eocene of France (Thaler, 1966). The oldest Asian glirid, *Glirulus zhoui* Wu et al., 2016, is known in the upper Oligocene of China (Wu et al., 2016). The occurrences of glirids in Asia remain rare. The occlusal pattern of glirid teeth is characterized by multiple parallel lophodont crests. In the extant genus *Graphiurus* Smuts, 1832, these extra crests, especially in upper molars, can be very irregular in shape and orientation, with various spurs, and we also observed this morphology in the new cricetid

*Corresponding authors

Published online 15 Jun 2021

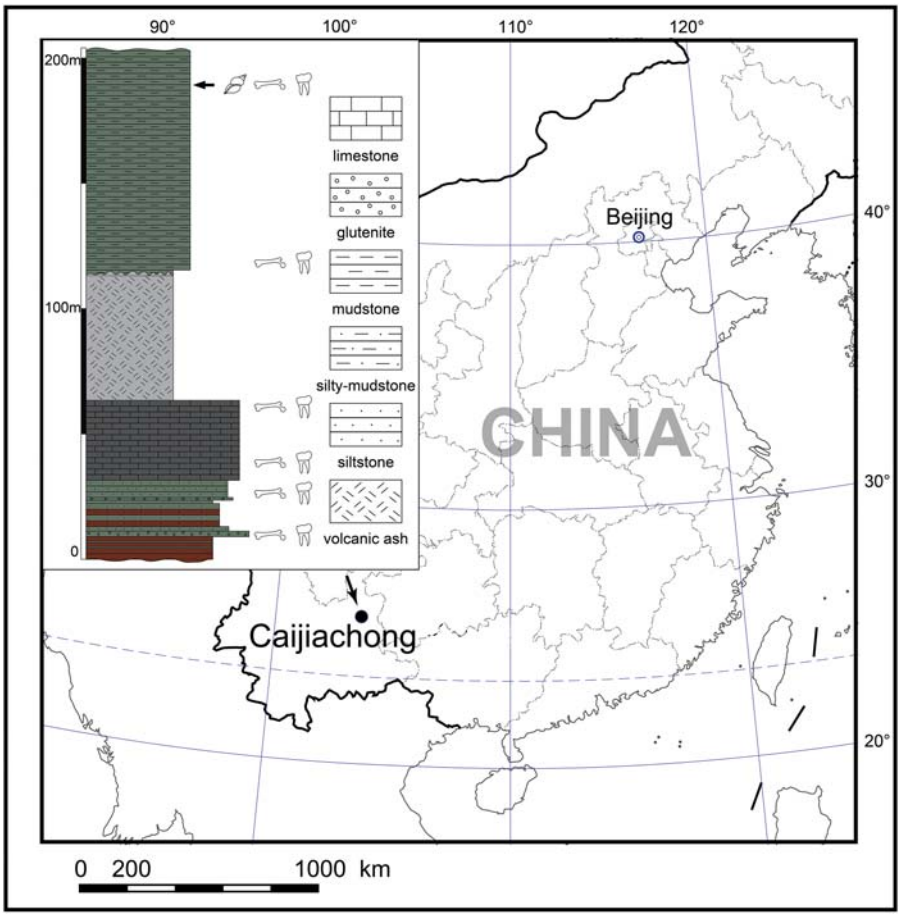

FIGURE 1. Location of the Caijiachong mammalian fossil sites in China. *Caecocricetodon yani* gen. et sp. nov. fossils were discovered from the highest fossiliferous layer (marked with black arrowhead).

reported here. Most of the extant glirids are arboreal and maintain a diet mostly composed of fruits and seeds. The molecular analyses (Blanga-Kanfi et al., 2009; Churakov et al., 2010) clearly indicate that Cricetidae s.l. and Gliridae are not closely related among Rodentia. As a result, these two families are referred to two different suborders of rodents (Blanga-Kanfi et al., 2009; Churakov et al., 2010). These suborders have recently been named Supramyomorpha, for the mouse-related clade including Cricetidae; and Eusciurida, for the squirrel-related clade including Gliridae (Flynn et al., 2019). The similarity between the new cricetid and glirids could be the result of convergent evolution of which controlling factors remain to be identified.

Dental terminology used in this study is after Maridet and Ni (2013). The upper molar paracone spur sensu Maridet and Ni (2013) is strong in the new species, so it is named distal arm of paracone in the descriptions below.

Institutional Abbreviations—IVPP, Institute of Vertebrate Paleontology and Paleoanthropology of the Chinese Academy of Sciences, Beijing, China.

Material and Methods

Fossiliferous sediments have been sampled from the lower Oligocene site 19 and 20 near the Caijiachong Village, Qujing County of Yunnan Province, China (Fig. 1). All specimens were collected by double screen-washing, the finer screen being 0.2 mm. The specimens are stored in the collections of IVPP. The specimen numbers include IVPP V 26103 and V 26104.1 to 26104.333.

The terminology used to score the characters in the phylogenetic analysis and describe the specimens follows Maridet and Ni (2013). Specimens were measured under the ZEN Pro 2012 system with a Zeiss stereo-microscope (Discovery V20, Carl Zeiss Microscopy GmbH, Jena, Germany), and were calibrated from digital calipers. The specimen images were produced using the 225 kV micro-CT facility at the Key Laboratory of Vertebrate Evolution and Human Origins of the Chinese Academy of Sciences. All these specimens were CT scanned with a beam energy of 140 kV and a flux of 100 μA at a detector resolution of 6.7 μm per pixel using a 360° rotation with a step size of 0.5° and an unfiltered aluminum reflection target. Three-dimensional reconstructions were produced in the VGStudio Max software 2.2 (www.volumegraphics.com).

SYSTEMATIC PALEONTOLOGY

Order RODENTIA Bowdich, 1821
Family CRICETIDAE Fischer von Waldheim, 1817
Genus *CAECOCRICETODON*, gen. nov.

Type Species—*Caecocricetodon yani*, sp. nov.
Included Species—The type species only.
Occurrence—Lower Oligocene, Yunnan Province, China.
Etymology—From the prefix 'Caeco', the Latin '*caecus*' meaning 'blind' or 'invisible' and the genus *Cricetodon* indicating a primitive morphology within the cricetid family. Caeco refers to the difficulty of distinguishing the classic cricetid-pattern of the molars due the multiple additional crests and spurs on the occlusal surface.

Diagnosis—Medium size cricetid with almost completely lophodont and low crowned cheek teeth. The mesolophs(ids) are variable and bear lots of extra crests or spurs. The mesostyle joins the distal arm of paracone and metacone ridge to form a labial cingulum in upper molars. The metalophulid is absent on m1, but complete on m2 and m3. The distal arms of protoconid and metaconid are distinct in lower molars. The metaconid ridge is long and forms the lingual cingulid in all lower molars.

CAECOCRICETODON YANI, sp. nov.
(Figs. 2–4)

Holotype—IVPP V 26103: right M1, 1.45 × 1.07 mm (length × width).

Hypodigm—IVPP V 26014.1–V 26014.63, M1, mean size: 1.43 × 1.09 mm; V 26014.64–V 26014.127, M2, mean size: 1.37 × 1.20 mm; V 26014.128–V 26014.163, M3, mean size: 1.21 × 1.17 mm; V 26014.164–V 26014.221, m1, mean size: 1.37 × 1.01 mm; V 26014.222–V 26014.280, m2, mean size: 1.42 × 1.11 mm; V 26014.281–V 26014.333, m3, mean size: 1.47 × 1.09 mm.

Etymology—Named after Mr. Zhou-Liang Yan in appreciation for his assistance in the fieldwork.

Diagnosis—As for the genus.

Type Locality—Caijiachong, Qujing, Yunnan Province, China; layer 19.

Measurements—see Table 1 and Supplemental Data 1.

Description

The dental morphology of this new species is very complex with noticeable variability. The description below focuses on the general pattern of the teeth, location and shape of the cusp (id)s and main crests (Figs. 3, 4). For all teeth described, numerous additional small crests or spurs are present on top of the

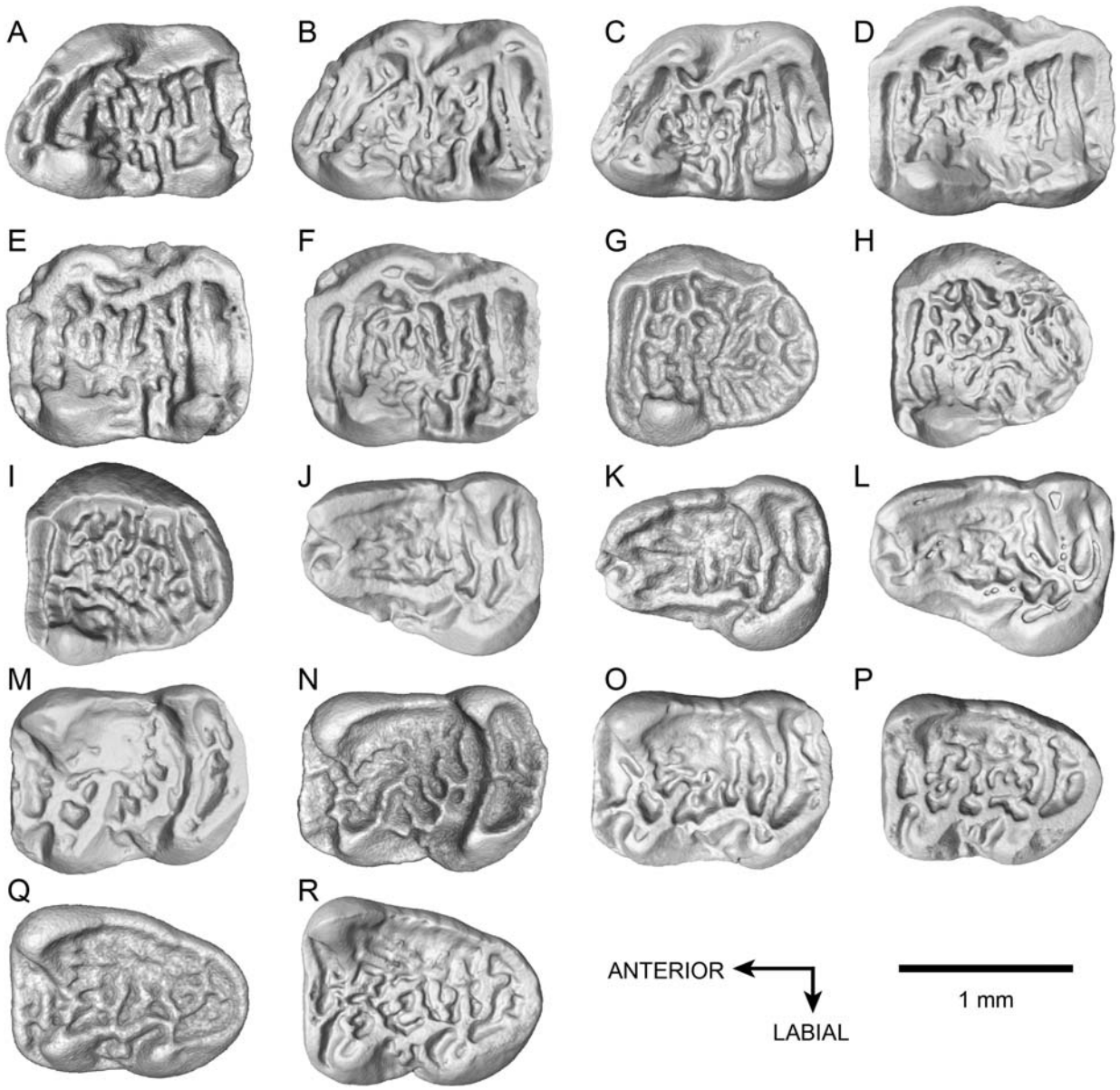

FIGURE 2. Upper and lower teeth of *Caecocricetodon yani*, gen. et sp. nov.: **A**, holotype, V 26103, right M1; **B**, V 26104.1, left M1; **C**, V 26104.2, right M1; **D**, V 26104.64, right M2; **E**, V 26104.65, left M2; **F**, V 26104.66, left M2; **G**, V 26104.128, left M3; **H**, V 26104.129, right M3; **I**, V 26104.130, right M3; **J**, V 26104.164, left m1; **K**, V 26104.165, right m1; **L**, V 26104.166, left m1; **M**, V 26104.222, left m2; **N**, V 26104.223, right m2; **O**, V 26104.224, left m2; **P**, V 26104.281, left m3; **Q**, V 26104.282, left m3; **R**, V 26104.283, left m3; B, E, F, G, K, N are reversed.

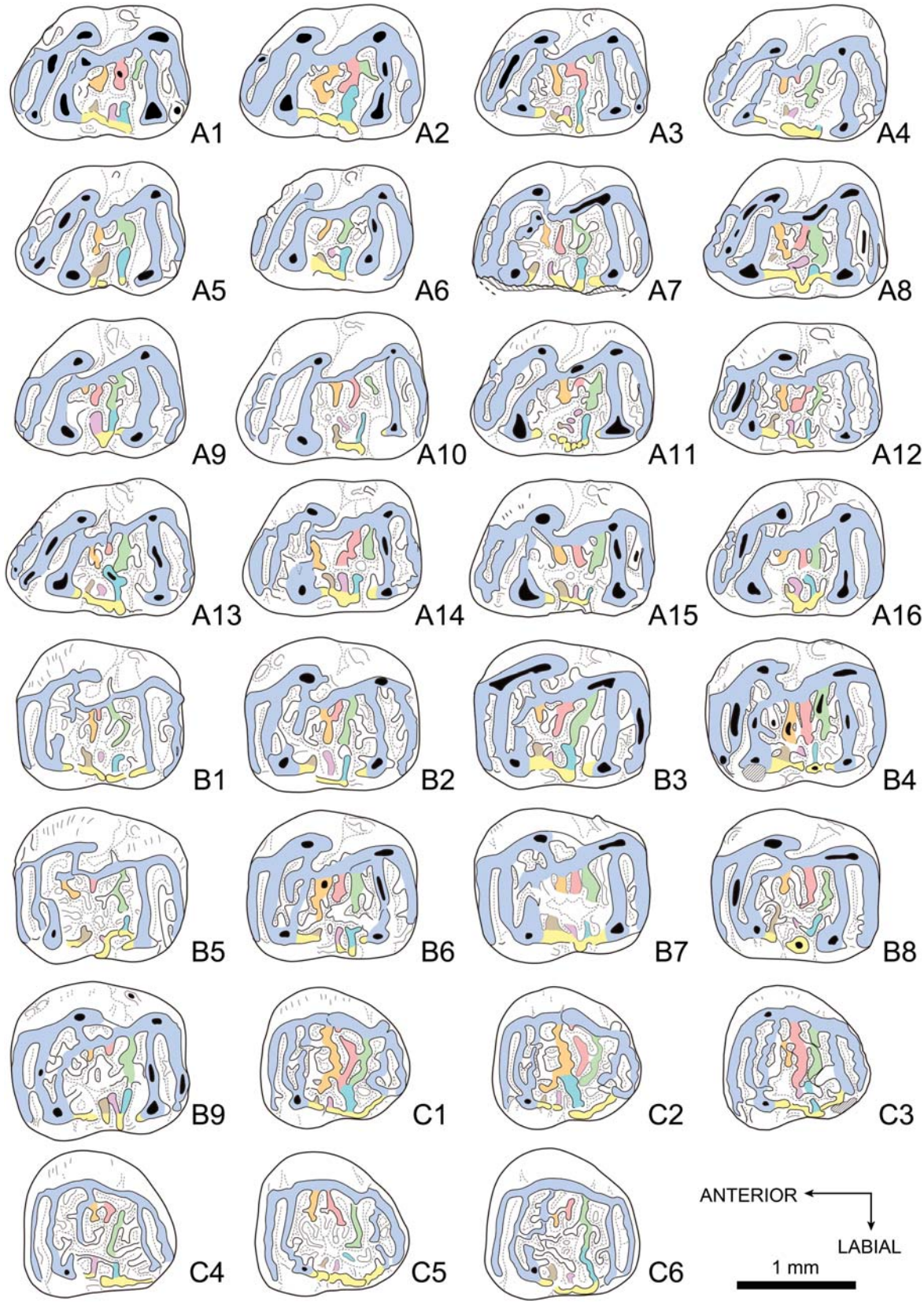

FIGURE 3. Colorized pattern for upper teeth of *Caecocricetodon yani*, gen. et sp. nov. **A1**, V 26104.44, right M1; **A2**, V 26104.51, left M1; **A3**, V 26104.12, right M1; **A4**, V 26104.50, left M1; **A5**, V 26104.45, right M1; **A6**, V 26104.53, left M1; **A7**, V 26104.13, left M1; **A8**, V 26104.10, left M1; **A9**, V 26104.47, left M1; **A10**, V 26104.54, right M1; **A11**, V 26104.19, left M1; **A12**, V 26104.33, right M1; **A13**, V 26104.48, right M1; **A14**, V 26104.8, right M1; **A15**, V 26104.16, right M1; **A16**, V 26104.39, left M1; **B1**, V 26104.74, left M2; **B2**, V 26104.69, left M2; **B3**, V 26104.77, left M2; **B4**, V 26104.81, right M2; **B5**, V 26104.75, left M2; **B6**, V 26164.70, left M2; **B7**, V 26104.79, right M2; **B8**, V 26104.83, left M2; **B9**, V 26104.85, right M2; **C1**, V 26104.139, right M3; **C2**, V 26104.141, right M3; **C3**, V 26104.142, right M3; **C4**, V 26104.144, left M3; **C5**, V 26104.145, right M3; **C6**, V 26104.134, right M3; A2, A4, A6, A7, A8, A9, A11, A16, B1, B2, B3, B5, B6, B8, and C4 are reversed. **Color reference**: **blue**, main lophs including anteroloph, mesial and distal protolophules, metalophule and posteroloph; **green**, **red**, **orange**, **sky blue**, **purple** and **brown**, mesolophs; **yellow**, labial cingulum.

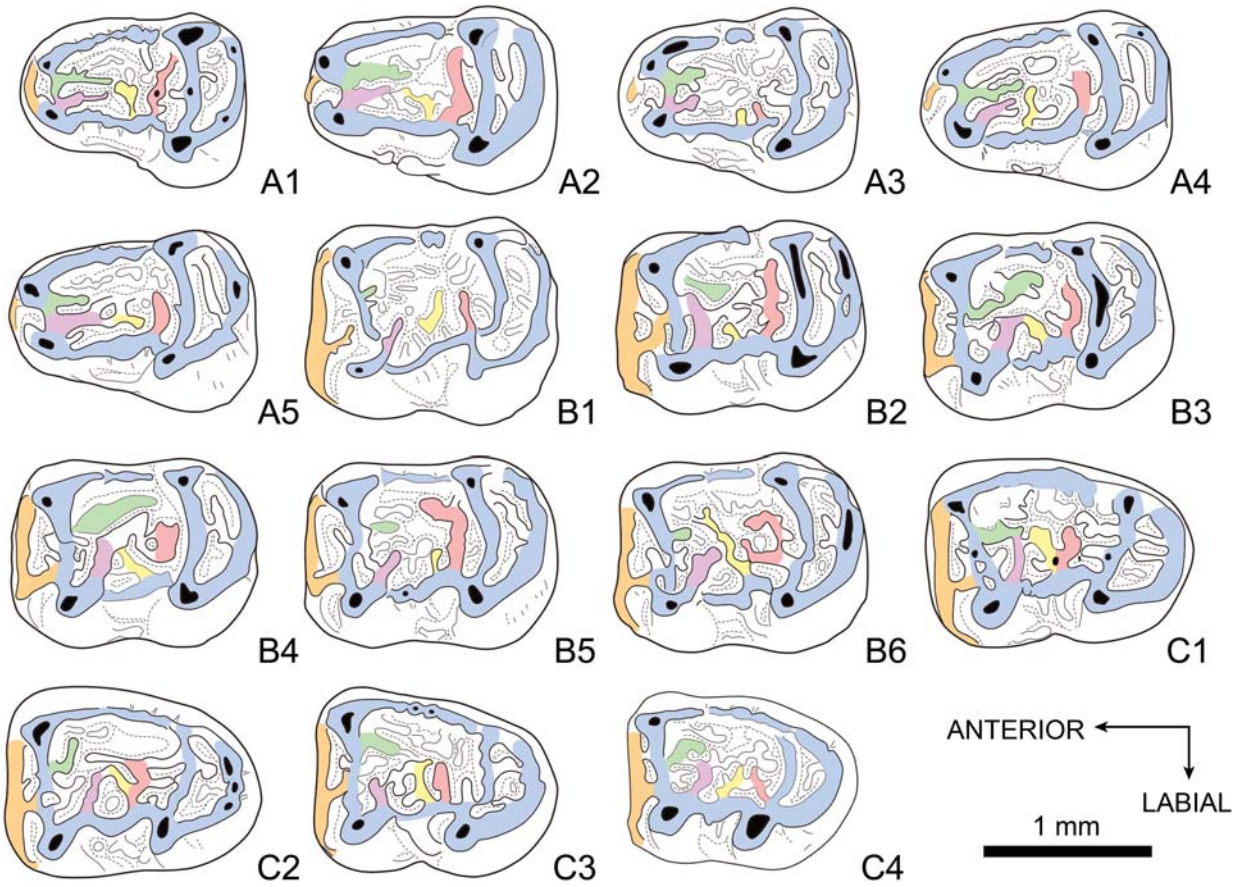

FIGURE 4. Colorized pattern for lower teeth of *Caecocricetodon yani*, gen.et sp. nov. **A1**, V 26104.169, right m1; **A2**, V 26104.170, left m1; **A3**, V 26104.172, right m1; **A4**, V 26104.174, right m1; **A5**, V 26104.175, left m1; **B1**, V 26104.226, right m2; **B2**, V 26104.230, right m2; **B3**, V 26104.233, left m2; **B4**, V 26104.236, right m2; **B5**, V 26104.242, left m2; **B6**, V 26104.246, left m2; **C1**, V 26104.285, right m3; **C2**, V 26104.288, left m3; **C3**, V 26104.297, left m3; **C4**, V 26104.301, left m3; A1, A3, A4, B1, B2, B4, and C1 are reversed. **Color reference**: **blue**, including lingual cingulid, ectolophid, hypolophulid and posterolophid; **green**, distal arm of metaconid; **purple**, distal arm of protoconid; **orange**, anterolophid; **yellow** and **red**, mesolophids.

TABLE 1. Molar measurements of *Caecocricetodon yani*, sp. nov. (in mm). **Abbreviations**: **CV**, coefficient of variation; **Max**, maximal value; **Min**, minimal value; **N**, number of specimens; **StD**, standard deviation.

	Length							Width						
	N	Min	Max	Mean		StD	CV	N	Min	Max	Mean		StD	CV
Site 19														
M1	38	1.38	1.51	1.44	±	0.038	2.63	39	1.02	1.16	1.09	±	0.034	3.07
M2	49	1.28	1.46	1.39	±	0.032	2.33	48	1.12	1.29	1.21	±	0.040	3.31
M3	27	1.10	1.35	1.23	±	0.059	4.82	26	1.13	1.27	1.18	±	0.035	2.99
m1	42	1.29	1.47	1.39	±	0.037	2.64	42	0.97	1.10	1.04	±	0.034	3.27
m2	46	1.28	1.49	1.43	±	0.037	2.61	46	0.99	1.16	1.11	±	0.036	3.24
m3	35	1.32	1.60	1.48	±	0.073	4.96	35	0.95	1.19	1.08	±	0.045	4.21
Site 20														
M1	22	1.29	1.55	1.41	±	0.076	5.35	22	0.97	1.19	1.09	±	0.052	4.82
M2	14	1.19	1.35	1.29	±	0.045	3.49	14	1.11	1.25	1.18	±	0.047	4.00
M3	8	1.05	1.22	1.15	±	0.051	4.44	8	1.07	1.20	1.16	±	0.048	4.10
m1	15	1.19	1.42	1.31	±	0.055	4.21	15	0.87	1.02	0.95	±	0.040	4.21
m2	10	1.30	1.44	1.38	±	0.044	3.21	10	1.02	1.17	1.10	±	0.052	4.70
m3	11	1.35	1.57	1.43	±	0.066	4.61	12	1.03	1.26	1.11	±	0.062	5.55

general pattern. The morphological variation of those small crests and spurs seems unpredictable from one tooth to another and produces a variety of connections, making each tooth morphologically unique.

Upper Dentition(Figs. 2A-I, 3)—M1 is trapezoidal and with a slightly concave occlusal surface. The single anterocone is usually small and located on the labial side of the anteroloph, easier to observe in some specimens (e.g., Fig. 3A1, A5). The anteroloph originates from the lingual side of the tooth extending anterolabially but not reaching the labial border. It is incomplete in some specimens (such as the holotype). The anterolophule presents both labially and lingually. It connects to the anteroloph and

mesial protolophule (also called protolophule I). However, in some specimens, the anterolophule is absent. The anteroloph can also connect to the protolophule through the end of the labial side of the anteroloph. Both protolophules, mesial and distal, are parallel to the anteroloph. As opposed to the distal protolophule (protolophule II), the mesial protolophule is complete and connects to the anteroloph through the anterolophule, the labial side of the anteroloph or both of them. The distal protolophule (protolophule II) is frequently interrupted, which results in the valley between the two protolophules being connected to the mesosinus. The protoconule is distinct and lies on the mesial protolophule (protolophule I) in some specimens. The distal arm of the protocone is sometimes elongated, but never reaches the entoloph. The paracone is slightly anterior to the protocone, it is the strongest cusp with a spear shape and the distal arm of the paracone usually extends backward and connects with the mesoloph or the mesostyle. The entoloph is robust and posterolingually oriented. The entomesoloph is absent. However, there are two or three mesolophs in the mesosinusid. The mesolophs display strong variations in their length, orientation and division. They bear several spurs, which sometimes connect to other main lophs. The mesostyle spurs join with the mesolophs on the labial side of tooth. The mesostyle is distinct and usually forms a labial cingulum which closes the mesosinus. The metalophule connects to the middle part of hypocone and extends transversely towards the metacone, sometimes being slightly inclined. The metacone ridge can be well developed. There is an extra loph developed from the middle of the posteroloph, similar to the hypoconid hind arm in lower molars. It extends in the posterosinus and reaches the labial border in some specimens.

M2 is a little larger than M1. The occlusal view of M2 is rectangular, with the mesial part sometimes slightly wider than the distal part. The anteroloph and protolophules are all transverse. The anterocone is weak and only a tiny cusp can be seen on the labial side of the anteroloph. The anterolophule is located in the lingual side of the tooth and connects to the labial side of the protocone. The anterosinus is always opened labially. As opposed to M1, the mesial protolophule connects with the mesial part of protocone and the paracone. The distal protolophule is normally incomplete. It develops from the middle part of protocone and extends posterolabially. The distal protolophule displays a noticeable variability. It can be interrupted in the middle or bears some spurs in the valley between the two protolophules. The protocone and paracone are much stronger than on M1. The distal arm of protocone is more developed and elongated posterolabially. In some specimens, the entomesoloph is present in the middle part of the entoloph and connects with the distal arm of the protocone, forming a round fossette. The rest of the M2 has two or three mesolophs with a strong variability as on M1. As on M1, there is also an extra crest developed from the posteroloph and extending in the posterosinus.

M3 is subtriangular with a strongly reduced lingual side distally. The anteroloph and anterolophule are similar to M2. The anterosinus is always open in its labial side. Proportionally, the transverse anteroloph is longer than on M2. But, the protolophules, metalophule and posteroloph are much thinner than those of M1 and M2. Both of the protolophules and metalophule are more sinuous than on M1 and M2. The paracone is the only distinct cusp on M3. The other cusps are weak and crest-like. The protocone is combined with the entoloph and forms a round lingual wall. The entomesoloph is absent. The mesolophs are slightly thinner than those on M1 and M2, but still with a strong variability. The labial cingulum is weak but generally complete. It connects to the distal arm of the paracone mesially and the posteroloph labially. The extra crest in the posterosinus is rare and present only in some specimens. The posteroloph is no longer transverse; instead, it forms a round distal wall and connects with the metalophule in the labial side.

Lower Dentition (Figs. 2J-R, 4)—The mesial part of m1 is much narrower than the distal part. The anteroconid is weak or absent. When present, it is close to the protoconid and even connects with protoconid through anterolophulid in some specimens. The metalophulid is absent. Two mesiodistal crests in the middle of the mesial part of the tooth are considered as the distal arms of protoconid and metaconid, respectively. They connect to each other mesially, occasionally with some tiny spurs distally. The metaconid ridge and the ectolophid are complete, parallel to each other and slightly oblique, forming the lingual cingulid. Sometimes, the metaconid ridge is not connected with the entoconid, whereas there is a weak and low connection between the ectolophid and the hypoconid. The ectomesolophid is absent. As for the mesolophs in upper molars, mesolophids also have a noticeable variability. Two weak transverse mesolophids can be observed. They originate from the ectolophid towards the lingual side and have spurs or connect to other crests forming a unique pattern for each tooth. Both the hypoconid and the entoconid are well developed on m1. The hypolophulid is complete and connects with the mesial part of these two cusps. The distal arm of the hypoconid is variable and enclosed in a fossette delimited by the hypolophulid and the posterolophid.

The m2 is slightly longer than m1, but wider in its mesial part. The anterolophid is well developed and the anteroconid is not distinct. Labially, the anterolophulid connects with the anterolophid and the transverse metalophulid I. Unlike m1, the metalophulid is always complete and slightly bent backward. The distal arm of the protoconid is transverse and slightly oblique (mesiodistal on m1). It disconnects to the distal arm of the metaconid. The distal arm of the metaconid is similar to that of m1. It could be either weakly or well developed and originates from the metalophulid. The rest of the distal part of m2 is similar to m1. The mesolophids are variable in the central valley, with lots of extra crests or spurs. The well-developed hypolophulid and posterolophid enclose the posterosinusid in some cases. The distal arm of hypoconid starts from the middle of posterolophid and extends to the lingual side along the sinusid.

The m3 is similar to the m2 in size. The distal part of m3 is narrower than m2. The only difference between m2 and m3 is in their distal parts. The hypolophulid is noticeably shorter than the metalophulid, whereas they are of equivalent length on m2. The protoconid, metaconid and hypoconid are developed as on m1 and m2, but the entoconid is much weaker. The posterolophid is strongly reduced in both lingual and labial sides and tends to form a round wall distally. The posterosinusid is usually closed and the distal arm of hypoconid is weaker and variable.

PHYLOGENETIC ANALYSIS

Our phylogenetic analysis is based on an updated version of the data matrix initially published by Maridet and Ni (2013). We combined two characters from their matrix (19: M1, presence of anterocone; 20: M1, size different between the lingual and labial parts of the divided anterocone) into one character with four states to describe the different type of anterocone: 0, absent; 1, simple, undivided; 2, divided, size subequal; 3, divided, size different. Considering their character 19 is unordered but 20 is ordered, here we use step-matrix method to order this new character. From 0 to 1 by one step; from 0 to 2 or 3 by two steps; from 1 to 0, 2 or 3 by one step; from 2(3) to 0 by two steps; from 2(3) to 1 or 3(2) by one step. Four new unordered characters are added into the new matrix for describing the presence of mesoloph(id) and ectomesolophid in cheek teeth (see Supplemental Data 2, 3). Compared to the initial analysis (Maridet and Ni, 2013), in order to focus on the relationships between Paleogene stem cricetids, five Neogene taxa are excluded

in the present analysis: *Deperetomys intermedius* de Bruijn, Ünay, Sarac and Klein Hofmeijer, 1987, *Enginia gertcheki* de Bruijn and von Koenigswald, 1994, *Meteamys alpani* de Bruijn, Ünay, van den Hoek Ostende and Saraç, 1992, *Mirabella tuberosa* de Bruijn, Ünay, Sarac and Klein Hofmeijer, 1987 and *Muhsinia steffensi* de Bruijn, Ünay, van den Hoek Ostende and Saraç, 1992.

Parsimony analysis was performed by PAUP* 4.0a167 (Swofford, 1998), with heuristic search, TBR branch-swapping, and random addition sequence for 1000 replicates (see Supplemental Data 4, 5). Our strict consensus tree (Fig. 5) is generated by six equally most parsimonious trees (tree length = 234, CI = 0.385, RI = 0.599). The relationships between the basal clades are well resolved in our analysis. *Caecocricetodon* forms a monophyletic group with *Paracricetodon* Schaub, 1925 and *Trakymys* Ünay-Bayraktar, 1989. Additionally, we used the age of each taxon to do the Bayesian analysis by Tip Dating method (see Supplemental Data 6, 7). The analysis was performed in MrBayes 3.2 (Ronquist et al., 2012). The result of the basal group is the same as in the parsimony analysis (see Supplemental Data 8). Although the relationships between the derived taxa are still unresolved, the present analyses may provide some guidelines for the future work.

The monophyly of *Caeocricetodon* and Paracricetodontinae Mein and Freudenthal, 1971 are well supported in our analysis, and the new genus represents the most basal taxon of the Paracricetodontinae clade. Here we therefore propose to refer *Caecocricetodon* to the subfamily Paracricetodontinae. Meanwhile, *Pappocricetodon recunensis* (the type species of the genus) is now grouped with *Caecocricetodon*, *Paracricetodon* and *Trakymys*, though *Pappocricetodon* still remains polyphyletic. *Caenocricetodon* might highlight a new phylogenetic relationship of *Pappocricetodon* with *Paracricetodon* and *Trakymys* that was

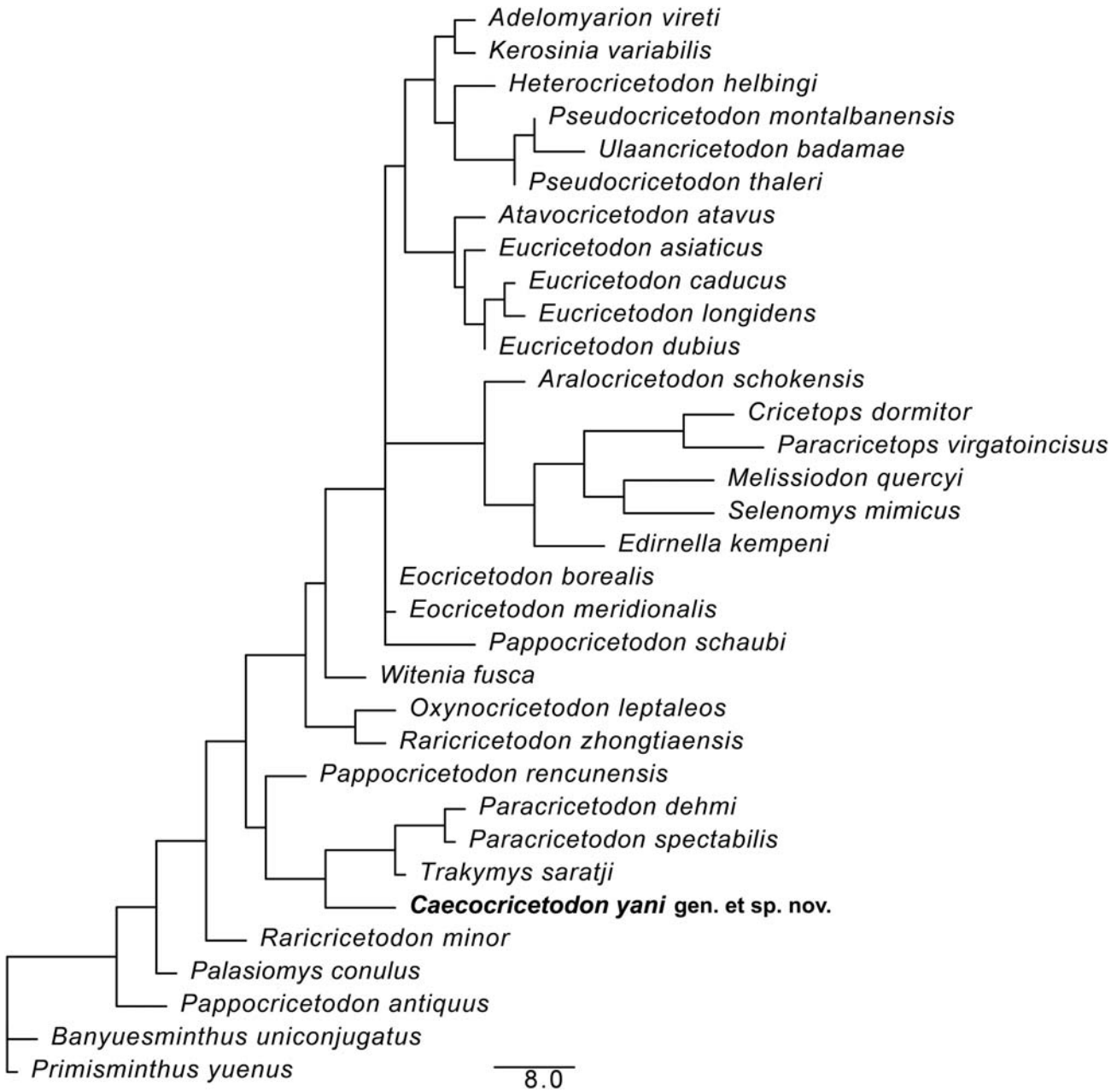

FIGURE 5. Result of the phylogenetic analysis, with the strict consensus tree of six most parsimonious trees. Scale bar equals 8 character changes.

not detected in previous phylogenetic analysis (Gomes Rodrigues et al. 2010; Maridet and Ni, 2013).

DISCUSSION

Caecocricetodon differs from any stem or crown cricetids known so far by the peculiar morphology of its cheek teeth. Both upper and lower molars are almost completely lophodont, with low crown, and a complicated pattern due to numerous and very variable crests and spurs. *Ulaancricetodon badamae* Daxner-Höck, 2000, from the early Oligocene of northern Asia, shares with *Caecocricetodon*, but to a lesser extent, a less lophodont, low crown pattern. *Caecocricetodon* presents morphology superficially similar to that of glirids, in which the cheek teeth all have a low crown and a complex lophodont pattern. The combination of numerous crests with complex spurs is characteristic for the living and fossil glirids, although some extant glirids (e.g., *Graphiurus lorraineus* Dollman, 1910) or extinct ones (e.g., *Glamys umbriae* Freudenthal, 2004) present a less complex occlusal pattern. However, except for this complex pattern, *Caecocricetodon* retains the morphological characteristics of cricetids s.l. with distinct differences in the shape of molars and the orientation of the main crests(ids) from glirids. Upper and lower first molars are indeed more elongated (as opposed to a square shape in glirids) and display no anterior contact surface which indicates the absence of P4 and p4. The screen-washing with the lower mesh size of 0.2 mm confirms the absence of P4 and p4 in sampled sediments. Additionally, both upper and lower first molars possess respectively an anterocone and an anteroconid which is never observed in glirids. Upper and lower molars all display respectively an entoloph and an ectolophid, while the transversal crest of these joining the pair of anterior and posterior cusp(id)s is also never observed in glirids (Fig. 6).

Like extant glirids (Fig. 6), but different from the other cricetids from the same area (such as *Cricetops* and *Paracricetops* Maridet and Ni, 2013; Li et al., 2016), *Caecocricetodon* has a low tooth crown with complex and lophodont tooth cusp-ridge pattern. This complex tooth pattern must indicate an adaptive pattern totally different from all the other early Oligocene cricetids, and probably implies a very low or inexistent abrasive component in the diet. Most extant glirids are arboreal (Novak, 1999). Even the most terrestrial species, such as *Eliomys* Wagner, 1840, *Graphiurus*, and *Myomimus* Ognev, 1924, live in a forest habitat (Novak, 1999). Unlike hypsodont mammals, which usually live in an open environment and are adapted to grazing grass associated with abrasive materials such as dust and sand (Kovalevsky, 1873; Osborn, 1910; Matthew, 1926; Fortelius and Solounias, 2000), low-crowned glirids are omnivores, feeding preferentially on fruit, nuts, eggs, small invertebrates, and more rarely other small vertebrates (Vaughan et al., 2000). A similar environment (with low dust and sand covering) and similar diet can be hypothesized for *Caecocricetodon*, given its dental pattern is very similar to those of dormice. This interpretation for the paleoenvironment of *Caecocricetodon* is consistent with the other small mammals previously described from the same locality, which also support an environment dominated by forest vegetation (e.g., Maridet and Ni, 2013; Li et al., 2016; Ni et al., 2016).

The highly complex occlusal surface with numerous crests, complex ridge connections and their sinuous shape in *Caecocricetodon* is unique. Famoso et al. (2013) studied the implication of the occlusal enamel complexity in ungulates. As part of the morphological complexity, the occlusal enamel bands lead to resistance for grinding against the opposing tooth (upper to lower). Although the enamel bands of ungulates are not really equivalent to the crests of our specimens, a similar mechanical advantage can be hypothesized. Also, part of the morphological complexity, cingulums and cingulids are

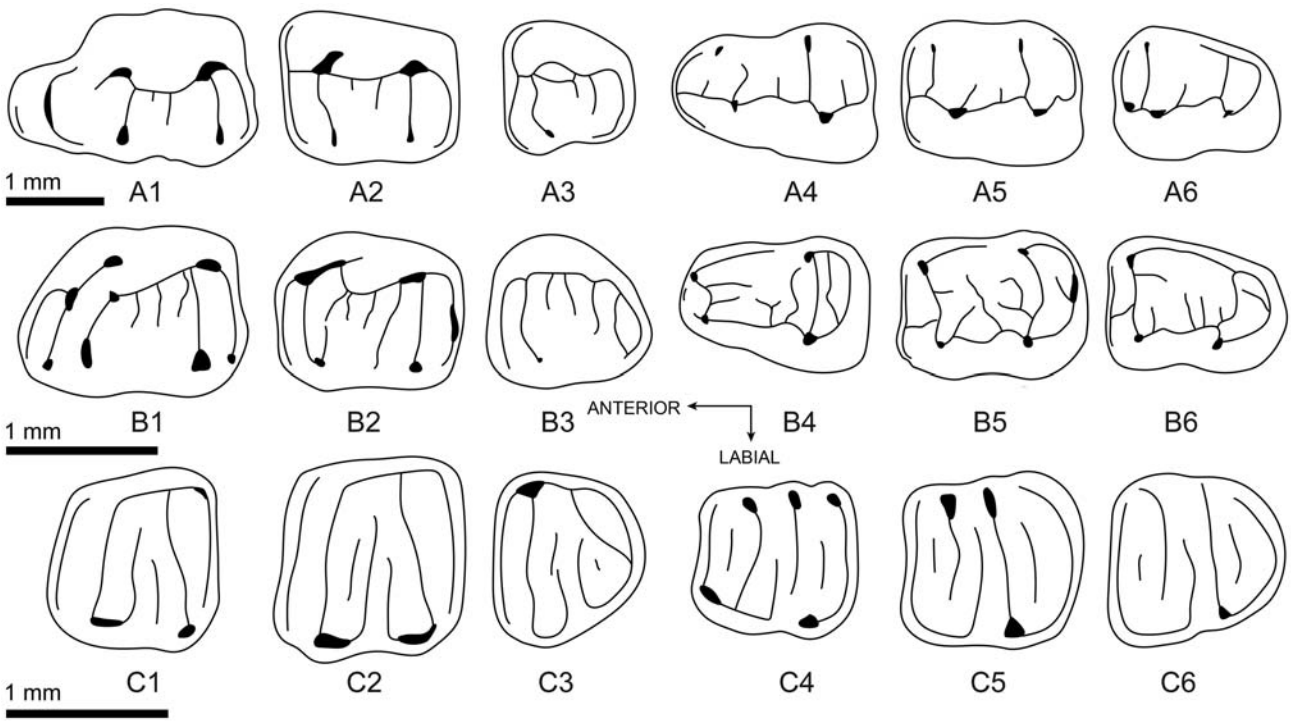

FIGURE 6. Comparison of molars among the Early Oligocene rodents. *Eucricetodon caducus* Shevyreva, 1967 (Cricetidae): **A1–A3**, M1–M3, **A4–A6**, m1–m3; *Caecocricetodon yani*, gen. et sp. nov. (Cricetidae): **B1–B3**, M1–M3, **B4–B6**, m1–m3; *Microdyromys misonnei* Vianey-Liaud, 1994 (Gliridae): **C1–C3**, M1–M3, **C4–C6**, m1–m3.

classically thought to be related to protecting gingiva (Kermack et al., 1968; Hillson, 2005). However, more recently, Anderson et al. (2011) used 3D models to analyze the effect of cingulums and cingulids on strain patterns in tooth enamel. They implied that the development of the lower molar lingual cingulid and the upper molar labial cingulum not only provides protection, but also has a possible functional advantage related to the reduction of strain. The extra low crests observed in our specimens may have the same function as the cingulum and cingulid: to reduce the strains on the main crests. This better resistance and reduced strain of teeth could be an adaptation to hard, but not abrasive, components of diet such as a higher proportion of seeds, fruit pits, or chitin exoskeletons of small arthropods, as opposed to other cricetids s.l.

During the Eocene–Oligocene transition, northern and central Asia may have undergone a significant aridification compared to the rest of Eurasia (Ramstein et al., 1997). As a result, in northern Asia, the climatic change led to a strong turnover where the late Eocene perissodactyl-dominant fauna was replaced by a rodent/lagomorph-dominant fauna at the beginning of the Oligocene, implying a drastic opening of landscapes (Meng and McKenna, 1998; Sun et al., 2014). By contrast, in southern Asia, the discovery of *Ptilocercus* (tree shrew) and diverse primates indicate that the tropical forest environment was still present in lower Oligocene (Li and Ni, 2016; Ni et al., 2016). Likewise, in Europe based on fossil plants, the mixed deciduous evergreen forests indicate a warm seasonal climate and the preservation of partly wet and closed vegetation at the beginning of the Oligocene (Collinson and Hooker, 1987; Collinson, 1992; Prothero, 1994).

Fossil glirids are abundant in Europe, but not present in the Asian mammalian fossil records until the late Oligocene (Maridet et al., 2011). *Caecocricetodon*, with their peculiar dental morphology, probably convergently evolved the dental adaptation morphology of Gliridae, and occupied an ecological niche similar to that of glirids in Europe at the same time. Based on the ecology of extant glirids, and in accordance with both the paleoenvironments of southern Asia and Europe at the beginning of the Oligocene, we propose that this ecological niche might have been linked to the conservation of partly wet and closed landscapes and the specific associated diet.

ACKNOWLEDGMENTS

We are grateful to Y.-M. Hou for CT scanning. G.-Z. Wang, R. Li and C.-M. Zhu sorted the concentrates of the screen washing. This project has been supported by the Strategic Priority Research Program of Chinese Academy of Sciences (XDA20070203-XDB26030300-XDA19050100, to X.N.), the National Natural Science Foundation of China (41888101-41988101-41625005, to X.N.), and two Swiss National Science Foundation (n°200021_162359 to X.L. and O.M.; n° CKSP_190584 to O.M.). We are also thankful to L. L. Jacobs, L. J. Flynn and Y. Kimura for helpful comments on successive versions of this paper.

ORCID

Xijun Ni http://orcid.org/0000-0002-4328-8695
Olivier Maridet http://orcid.org/0000-0002-0956-0712

LITERATURE CITED

Anderson, P. S., P. G. Gill, and E. J. Rayfield. 2011. Modeling the effects of cingula structure on strain patterns and potential fracture in tooth enamel. Journal of Morphology 272:50–65.

Blanga-Kanfi, S., H. Miranda, O. Penn, T. Pupko, R. W. DeBry, and D. Huchon. 2009. Rodent phylogeny revised: analysis of six nuclear genes from all major rodent clades. BMC Evolutionary Biology 9:71.

Bowdich, T. E. 1821. An Analysis of the Natural Classifications of Mammalia, for the Use of Students and Travellers. J. Smith, Paris, 115 pp.

Churakov, G., M. K. Sadasivuni, K. R. Rosenbloom, D. Huchon, J. Brosius, and J. Schmitz. 2010. Rodent evolution: back to the root. Molecular Biology and Evolution 27:1315–1326.

Collinson, M. E. 1992. Vegetational and floristic changes around the Eocene/Oligocene boundary in western and central Europe. Princeton University Press, 430 pp.

Collinson, M. E., and J. J. Hooker. 1987. Vegetational and mammalian faunal changes in the Early Tertiary of southern England. In International Congress of Systematics and Evolutionary Biology 3:259–304.

Daxner-Höck, G. 2000. *Ulaancricetodon badamae* n. gen., n. sp. (Mammalia, Rodentia, Cricetidae) from the Valley of Lakes in Central Mongolia. Paläontologische Zeitschrift 74:215–225.

De Bruijn, H., and W. von Koenigswald. 1994. Early Miocene rodent faunas from eastern Mediterranean area. Part V. The genus *Enginia* (Muroidea) with a discussion of the structure of the incisor enamel. Proceedings van de Koninklijke Nederlandse Akademie van Wetenschappen 97:381–405.

De Bruijn, H., E. Ünay, G. Sarac¸ and G. Klein Hofmeijer. 1987. An unusual new eucricetodontine from the Lower Miocene of the Eastern Mediterranean. Proceedings of the Koninklijke Nederlandse Akademie van Wetenschappen 90:119–132.

De Bruijn, H., E. Ünay, L. W. van den Hoek Ostende, and G. Saraç. 1992. A new association of small mammals from the lowermost Lower Miocene of Central Anatolia. Geobios 25:651–670.

Dollman, G. 1910. Two new African mammals. Annals and Magazine of Natural History 8:266–230.

Famoso, N. A., R. S. Feranec, and E. B. Davis. 2013. Occlusal enamel complexity and its implications for lophodonty, hypsodony, body mass, and diet in extinct and extant ungulates. Palaeogeography, Palaeoclimatology, Palaeoecology 387:211–216.

Fischer von Waldheim, J. G. 1817. Adversaria zoologica. Mémoires de la Société Impériale des Naturalistes de Moscou 5:357–471.

Flynn, L. J., Jacobs, L. L., Kimura, Y. and E. H. Lindsay. 2019. Rodent Suborders. Fossil Imprint 75:292–298.

Fortelius, M., and N. Solounias. 2000. Functional characterization of ungulate molars using the abrasion-attrition wear gradient: a new method for reconstructing paleodiets. American Museum Novitates 3301:1–36.

Freudenthal, M. 2004. Gliridae (Rodentia, Mammalia) from the Eocene and Oligocene of the Sierra Palomera (Teruel, Spain). Treballs del Museu de Geología de Barcelona 12:97–173.

Gomes Rodrigues, H., Marivaux, L., and M. Vianey-Liaud. 2010. Phylogeny and systematic revision of Eocene Cricetidae (Rodentia, Mammalia) from Central and East Asia: on the origin of cricetid rodents. Journal of Zoological Systematics and Evolutionary Research 48:259–268.

Hillson S. 2005. Teeth. 2nd edition. Cambridge, United Kingdom, Cambridge University Press, 173 pp.

Kermack, D. M., K. A. Kermack, and F. Mussett. 1968. The Welsh pantothere *Kuehneotherium praecursoris*. Zoological Journal of the Linnean Society 47:407–423.

Kovalevsky, W. 1873. On the osteology of the hypopotamidae, by Dr. Kowalevsky, communicated by Professor Huxley. Philosophical Transactions of the Royal Society of London 163:19–94.

Li, L.-Z., X.-N. Ni, X.-Y. Lu, and Q. Li. 2016. First record of *Cricetops* rodent in the Oligocene of southwestern China. Historical Biology 29:488–494.

Li, Q. and X.-J. Ni. 2016. An early Oligocene fossil demonstrates treeshrews are slowly evolving "living fossils". Scientific reports 6:18627.

Maridet, O., and X.-J. Ni. 2013. A new cricetid rodent from the early Oligocene of Yunnan, China, and its evolutionary implications for early Eurasian cricetids. Journal of Vertebrate Paleontology 33:185–194.

Maridet, O., W.-Y. Wu, J. Ye, X.-J. Ni, and J. Meng. 2011. New discoveries of glirids and eomyids (Mammalia, Rodentia) in the Early Miocene of the Junggar basin (Northern Xinjiang province, China). Swiss Journal of Palaeontology 130:315–323.

Matthew, W. D. 1926. The evolution of the horse: a record and its interpretation. Quarterly Review of Biology 1:139–185.

Mein, P., and M. Freudenthal. 1971. Une nouvelle classification des Cricetidae (Rodentia, Mammalia) du Tertiaire d'Europe. Scripta Geologica 2:1–37.
Meng, J., and M. C. McKenna. 1998. Faunal turnovers of Palaeogene mammals from the Mongolian Plateau. Nature 394:364–367.
Ni, X.-J., Q. Li, L.-Z. Li, and K. C. Beard. 2016. Oligocene primates from China reveal divergence between African and Asian primate evolution. Science 352:673–677.
Novak, R. 1999. Walker's Mammals of the World, Sixth Edition. Baltimore and London: The Johns Hopkins University Press, 2015 pp.
Ognev, S. I. 1924. Nature and sport in Ukraine, Kharkov. 1 pp.
Osborn, H. F. 1910. The age of mammals in Europe, Asia and North America. Macmillan, New York. 670 pp.
Prothero, D. R. 1994. The late Eocene-Oligocene extinctions. Annual Review of Earth and Planetary Sciences 22:145–165.
Ramstein, G., F. Fluteau, J. Besse, and S. Joussaume. 1997. Effect of orogeny, plate motion and land-sea distribution on Eurasian climate change over the past 30 million years. Nature 386:788–795.
Ronquist, F., M. Teslenko, P. van der Mark, D. L. Ayres, A. Darling, S. Höhna, B. Larget, L. Liu, M.A. Suchard, and J. P. Huelsenbeck. 2012. MRBAYES 3.2: Efficient Bayesian phylogenetic inference and model selection across a large model space. Systematic Biology 61:539–542.
Schaub, S. 1925. Die hamsterartigen Nagetiere des Tertiärs und ihre lebenden Verwandten. Abhandlungen der Schweizerischen Paläontologischen Gesellschaft 45:1–114.
Shevyreva, N. S. 1967. *Cricetodon* from middle Oligocene of central Kazakhstan. Paleontologicheskia Zhurnal 1967: 90–98. [in Russian]
Smuts, J. J. L. 1832. Dissertatio zoologica, enumerationem mammalium capensium. Cyfveer, 105 pp.
Sun, J.-M., X.-J. Ni, S.-D. Bi, W.-Y. Wu, J. Ye, J. Meng, and B. F. Windley. 2014. Synchronous turnover of flora, fauna, and climate at the Eocene–Oligocene Boundary in Asia. Scientific Reports 4:7463.
Swofford, D. L. 1998. PAUP*: Phylogenetic Analysis Using Parsimony (*and Other Methods), Version 4. Sinauer Associates, Sunderland, Massachusetts.
Thaler, L. 1966. Les Rongeurs fossiles du Bas-Languedoc dans leurs rapports avec l'Histoire des faunes et la Stratigraphie du Tertiaire d'Europe. Mem Mus Nat Hist Nat Paris C: 1–295.
Thomas, O. 1897. On the genera of rodents: an attempt to bring up to date the current arrangement of the order. Proceedings of the Zoological Society London X:50–76.
Tong, Y.-S. 1997. Middle Eocene small mammals from Liguanqiao basin of Henan province and Yuanqu basin of Shanxi province, central China. Paleontologica Sinica, New Series C 18:1–256.
Ünay, E. 1989. Rodents from the Middle Oligocene of Turkish Thrace. Utrecht Micropaleontological Bulletin, Special Publication 5:1–119.
Vaughan, T. A., J. M. Ryan, and N. J. Czaplewski. 2000. Mammalogy, 4th edition. Thomson Learning, New York, 565 pp.
Vianey-Liaud, M. 1994. La radiation des Gliridae (Rodentia) à l'Eocène supérieur en Europe Occidentale et sa descendance Oligocène. Münchner Geowissenschaftliche Abhandlungen A: 117–160.
Wagner, J. A. 1840. Beschreibung einiger neuer Nager. Abhandlungen der Bayerischen Akademie der Wissenschaften - Mathematisch-naturwissenschaftliche Klasse 3:173–218.
Wang, B.-Y., and M. R. Dawson. 1994. A primitive cricetid (Mammalia: Rodentia) from the middle Eocene of Jiangsu province, China. Annals of the Carnegie Museum 63:239–256.
Wu, W.-Y., J. Meng, J. Ye, X.-J. Ni, and S.-D. Bi. 2016. Restudy of the Late Oligocene dormice from northern Junggar Basin. Vertebrata PalAsiatica 54:36–50.

Submitted May 6, 2020; revisions received December 12, 2020;
accepted February 11, 2021.
Handling Editor: Edward Davis.